Cancer Nanotechnology

RESEARCH Open Access

Delivery of CXCL9/10/11 plasmid DNAs promotes the tumor-infiltration of T cells and synergizes with PD1 antibody for treating lung cancer

Yuxia Ma[1*†], Yi Liu[2†], Ying Zhi[1], Haibin Wang[1], Mei Yang[1], Jieting Niu[1], Li Zhao[1] and Pengsheng Wang[1]

*Correspondence: DrMayuxia@foxmail.com
†Yuxia Ma and Yi Liu contributed equally to this work
[1] Department of Internal Medicine, Cangzhou Central Hospital, 6 Xinhua WestRoad, Cangzhou 061001, Heibei, China
Full list of author information is available at the end of the article

Abstract

Background: Immune checkpoint blockade (ICB)-based cancer immunotherapy presents promising efficacy in cancer treatment. However, only a small portion of patients show responsiveness to the treatment, which is partially caused by limited tumor infiltration of T cells. Chemokines CXCL9, CXCL10 and CXCL11 bind to their receptor CXCR3 to regulate T cell invasion.

Methods: We delivered plasmids encoding CXCL9, CXCL10 and CXCL11 to tumor cells and tumor tissues using nanoparticles and investigated their effect on T cell invasion and infiltration. In addition, we applied these nanoparticles together with anti-PD-1 antibody, which is known to activate T cells and restore immune function against tumor cells. The anti-tumor effects were evaluated.

Results: Delivering plasmids encoding CXCL9, CXCL10 and CXCL11 by nanoparticles resulted in expression of these chemokines in both LLC cells and tumors. Expressing CXCL9, CXCL10 and CXCL11 promoted the infiltration of T cells in vitro and in vivo, as well as decreased the tumor size. Nanoparticles together with anti-PD-1 displayed the best anti-tumor effects.

Conclusions: Delivery of CXCL9/10/11 plasmids by nanoparticles promoted T cell infiltration in tumors and synergizes with the activity of anti-PD1 antibody.

Keywords: CXCL9/10/11, Infiltration, T cell, PD1, Cancer

Introduction

Lung cancer, also known as lung carcinoma, is a type of cancer with the highest incidence and mortality world-widely (Dela Cruz et al. 2011). There are two main categories of lung cancer: non-small cell lung cancer (NSCLC) and small cell lung cancer, and NSCLC accounts for 85% of lung cancers (Sosa Iglesias et al. 2018).

Nowadays, lung cancer treatments include surgical resection, chemotherapy, radiation, targeted therapy, immune therapy, and/or their combinations (Miller et al. 2016). Chemotherapy comprising 2 chemo drugs such as cisplatin, carboplatin, paclitaxel

(Taxol) and docetaxel (Taxotere) is often used to treat early stage lung cancer. However, drug resistance leads to therapeutic failure and results in tumor recurrence and progression (Kim 2016). In recent years, targeting immune checkpoints has become an effective strategy for anti-tumor immunotherapy. The development of immune checkpoint blocking (ICB) antibodies has become a hot spot in the global biopharmaceutical field. Ipilimumab (CTLA-4 monoclonal antibody), Pembrolizumab and Nivolumab (PD-1 monoclonal antibody), Atezolizumab and Avelumab (PD-L1 monoclonal antibody) have been approved to treat tumors including lung cancer (Massarelli et al. 2014). Immunotherapy targeting PD1/PDL1 has reached notable success in recent years (Jiang et al. 2019; Huang et al. 2020). However, the number of patients showing clinical response to PD1/PDL1 treatment is limited. The major reason of PD1/PDL1 inhibitor resistance is the low rate of tumor T cell infiltration (Bonaventura et al. 2019). Promoting T cell infiltration in tumor microenvironment could overcome the resistance to PD-L1 blockade (Tang et al. 2016).

Chemokines are small proteins which bind to their receptors to regulate cell trafficking (Luster 1998). The chemokine receptor CXCR3 is mainly expressed on $CD4^+$ and $CD8^+$ T cells. CXCR3 binds to its ligands CXCL9, CXCL10, and CXCL11 to regulate T cell migration (Groom and Luster 2011). Production of CXCR3 ligands by tumor cells recruits T cells and is associated with tumor suppression (Mikucki et al. 2015; Harlin et al. 2009; Luster and Leder 1993; Fujita et al. 2009). In addition, the intra-tumoral activity of CXCR3 is required for anti-PD-1 therapy efficacy (Chow et al. 2019). Therefore, upregulation of CXCL9, CXCL10, CXCL11 and CXCR3 should benefit the anti-tumor effects. Poly (β-amino ester) (PBAE) constitutes a novel class of biodegradable cationic polymers with many desirable properties to formulate nanoparticle-based form for the development of site-specific drug and gene delivery systems (Potineni et al. 2003). In this study, we utilized the PBAE nanoparticles containing plasmids encoding CXCL9, CXCL10, and CXCL11 to deliver these plasmids to tumor cells to induce chemokine expression, and investigated the potential anti-tumor effects of these nanoparticles.

Results

Preparation and characterization of PBAE/pDNA complex

First, we prepared the nanoparticles containing plasmids encoding CXCL9, CXCL10 and CXCL11 by mixing PBAE polymer and plasmids (Fig. 1A). The chemical structure and FTIR spectra of PBAE was presented in Additional file 1: Fig. S1A, B. PBAE/pDNA complex was generated by the interaction of positive PBAE and negative DNA. To determine the best binding ratio of PBAE and plasmids, we mixed plasmids and PBAE with different ratios and the binding efficiency was determined by electrophoresis. There was no free plasmid DNA detected in mixtures with ratio 1:5, 1:10 and 1:15 (Fig. 1B), indicating at these ratios all the plasmids were completed mixed with PBAE. We also found the stability and cytotoxicity of the PBAE/pDNA complex increased with increasing PBAE. Considering the stability and biosafety, we used 1:10 ratio to generate the nanoparticles. These nanoparticles showed hydrodynamic diameters around 100 nm which was measured by Malvern Zetasizer apparatus (Fig. 1C). The average hydrodynamic diameter of PBAE/pDNA complex A in DMEM medium (10% FBS) was around 105 nm with a small polydispersity index (PDI) value less than 0.2, and the surface potential was about

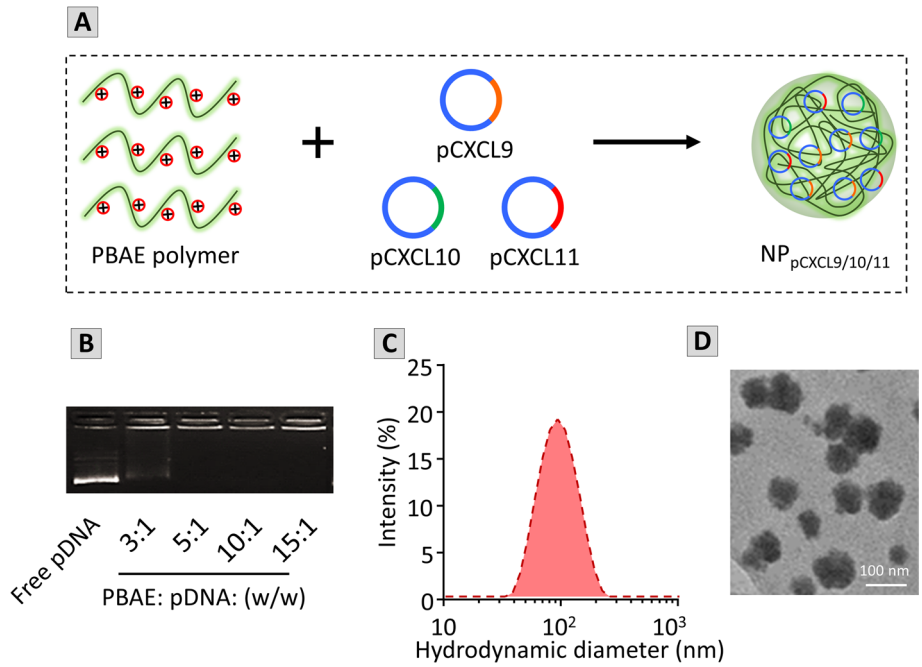

Fig. 1 Preparation and characterization of PBAE/pDNA complex. **A** Polymer 446, a type of poly (beta-amino esters) (PBAEs), could deliver plasmid DNA efficiently. Here, PBAE 446 was used to bind and deliver plasmids encoding CXCL9, CXCL10, and CXCL11. **B** PBAE 446 was 100% effective at binding plasmid DNA at 5, 10, and 15 w/w ratios of polymer to DNA, the ratio of 10 was selected for further study. **C** Nanoparticle hydrodynamic diameter. The PBAE/pDNA complex was formed at 10 w/w ratios of polymer to DNA. **D** Representative SEM (scanning electron microscope) images of PBAE/pDNA complex. Scale bar, 100 nm

14.5 mV. Scanning electron microscope (SEM) analysis revealed that the PBAE/pDNA complex exhibited a compact and spherical morphology with a rough surface (Fig. 1D). The hydrodynamic diameters of nanoparticles measured by dynamic light scattering (DLS) were also relatively larger than those observed by SEM.

Transfection of $NP_{pCXCL9/10/11}$ induces CXCL9/10/11 expression in murine LLC

Next, we treated LLC cells with nanoparticles to monitor the expression of nanoparticle plasmid-encoded proteins. Cloning vector pEGFP-N2 expressing enhanced green fluorescent protein (GFP) was used for examining the transfection efficacy of PBAE/DNA complex. Lipofectamine 2000 was used as positive control to evaluate the transfection efficacy of NPpCXCL9/10/11. As shown in Fig. 2A, B, in LLC cells treated with free pEGFP-N2 plasmids, there were minimal GFP-positive cells. LLC cells transfected with pEGFP-N2 using Lipofectamine ($Lipo_{pEGFP\text{-}N2}$) showed increased percentage of GFP-positive cells. In contrast, LLC cells treated with $NP_{pEGFP\text{-}N2}$ displayed the most intensive GFP signal and the highest percentage of GFP-positive cells, indicating $NP_{pEGFP\text{-}N2}$ exhibited the best efficiency to deliver plasmids. Consistently, we detected the highest protein levels of CXCL9, CXCL10 and CXCL11 in LLC cells treated with $NP_{pCXCL9/10/11}$ when compared to cells treated with free pCXCL9/10/11 or transfected with pCXCL9/10/11 using Lipofectamine ($Lipo_{pCXCL9/10/11}$) (Fig. 2C), indicating higher efficiency of NPpCXCL9/10/11 to deliver DNA into cells. Correspondingly, we observed

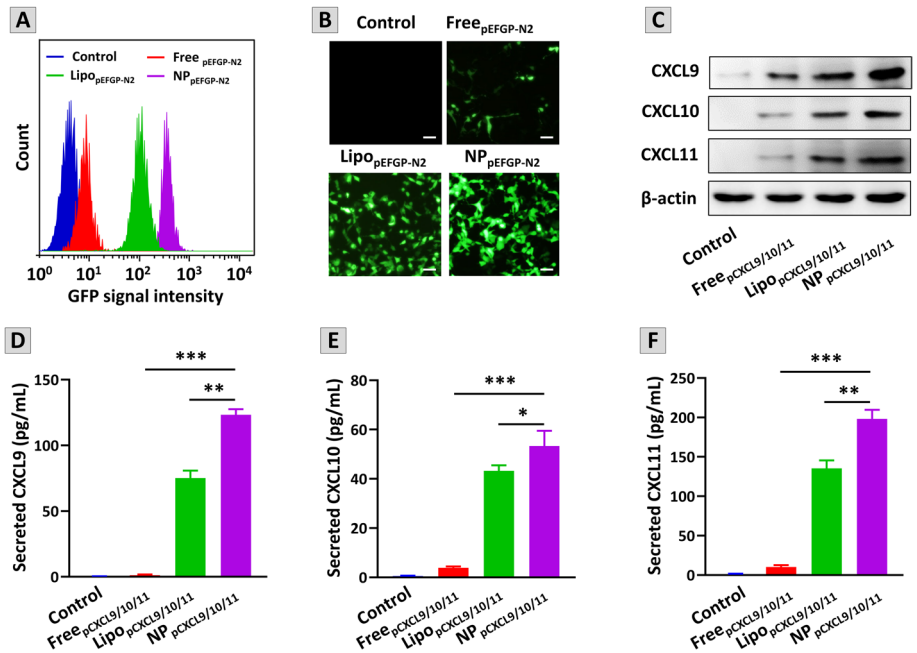

Fig. 2 NPpCXCL9/10/11 transfection induce expressions of CXCL9/10/11 in murine Lewis lung cancer (LLC) cells. LLC cells were transfected with PBAE/pDNA nanoplex containing pEGFP-N2, which encoding enhanced green fluorescence protein. The concentration of pEGFP-N2 was 2 μg/mL. $Free_{pEGFP\text{-}N2}$ and Lipofectamine $2000^{TM}{}_{pEGFP\text{-}N2}$ were set as controls. After 48 h transfection, the expression of GFP in LLC cells was examined by flow cytometry (**A**) and fluorescence microscope (**B**). LLC cells were transfected with PBAE/pDNA nanoplex containing pCXCL9, pCXCL10 and pCXCL11, the concentration of three plasmids was 0.67 μg/mL. After 48 h of transfection, the protein levels of CXCL9, CXCL10, and CXCL11 were examined by western blot (**C**). The concentrations of CXCL9 (**D**), CXCL10 (**E**), and CXCL11 (**F**) in the supernatant of LLC cells after 48 h of transfection. *$p < 0.05$, **$p < 0.01$, and ***$p < 0.001$

significantly increased levels of secreted CXCL9 (Fig. 2D), CXCL10 (Fig. 2E) and CXCL11 (Fig. 2F) in the cell culture supernatant of LLC cells treated with $NP_{pCXCL9/10/11}$ 48 h post transfection. In addition, transfection of PBAE/pDNA complex to mouse liver cell line NCTC 1469 cells and Lewis lung carcinoma cells (LLC) did not cause obvious cell toxicity (Additional file 1: Fig. S2), suggesting the biosafety of these Nanoparticles. Taken together, these results indicated that nanoparticles could efficiently deliver the plasmids to LLC cells and induce chemokine expression.

LLC cells expressing chemokines promoted the invasion of T cells in vitro

Next, we examined whether the chemokine-expressing LLC cells affected invasion of T cells. Both $CD4^+$ and $CD8^+$ T cells expressed CXCR3, the receptor of CXCL9, CXCL10 and CXCL11 (Fig. 3A, B). Then we tested the invasion of T cells using Transwell assay (Fig. 3C), where LLC cells were cultured in the lower compartment, while fluorescently labeled were cultured in the upper compartment. As CXCL9, CXCL10, CXCL11 together with their receptor CXCR3 mediated the invasion of T cells, transfected LLC cells secreting CXCL9, CXCL10, and CXCL11 could induce the invasion of T cells to the microporous membrane and enter the lower compartment. In co-culture of T cells together with normal LLC cells or LLC cells treated with free plasmids encoding

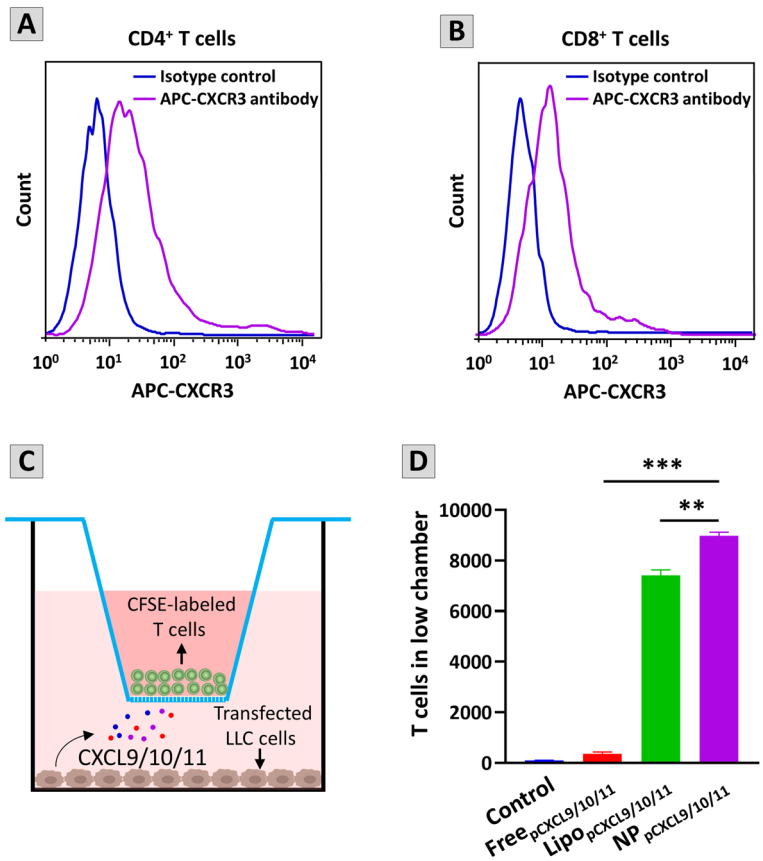

Fig. 3 Chemokines released by transfected LLC cells promote the invasion of T cells in vitro. The expressions of CXCR3 on CD4 + T cells (**A**) and CD8 + T cells (**B**) were examined by flow cytometry. T cells were isolated from the spleen and stained with APC labeled anti-CXCR3 antibody. CXCL9, CXCL10, CXCL11/CXCR3 axis mediate the invasion of T cells. **C** Transwell system was used to measure the invasion of T cells. 1×10^5 NPpCXCL9/10/11-transfected LLC cells and CFSE-labeled T cells were cultured in the lower and upper compartments, respectively. **D** Number of T cells in the lower compartment was examined 48 h later. Data are presents as mean ± S.D. *p < 0.05, **p < 0.01, and ***p < 0.001

CXCL9/10/11, there was minimal invasion of T cells to the bottom (Fig. 3D). In contrast, in the co-culture of T cells together with LLC cells treated with $Lipo_{pCXCL9/10/11}$, we detected significantly increased T cells in the bottom, indicating there was invasion of T cells. In addition, in the co-culture of T cells together with LLC cells treated with $NP_{pCXCL9/10/11}$, the T cells number in the bottom was significantly higher than that in the co-culture of T cells with LLC cells treated with $Lipo_{pCXCL9/10/11}$. Interestingly, LLC cells expressing CXCL9/10/11 together induced stronger T cell invasion when compared to LLC cells expressing any single chemokine (CXCL9, CXCL10 or CXCL11) (Additional file 1: Fig. S3), indicating stronger invasion of T cells in response to triple chemokines but not to a single chemokine. Collectively, these results demonstrated that expressing chemokines CXCL9 CXCL10 and CXCL11 promoted the T cell invasion.

$NP_{pCXCL9/10/11}$ exhibited anti-tumor effects in vivo

We continued to assess the effects of $NP_{pCXCL9/10/11}$ on tumor tissues in mice. We established the LLC tumor model and administrated $NP_{pCXCL9/10/11}$ to mice. The tumor

volume was monitored at different timepoints. The volume of tumor in mice without treatment increased in a time-dependent manner (Fig. 4A). Free pCXCL9/10/11 treatment did not affect the tumor volume. In contrast, the tumor volume was significantly

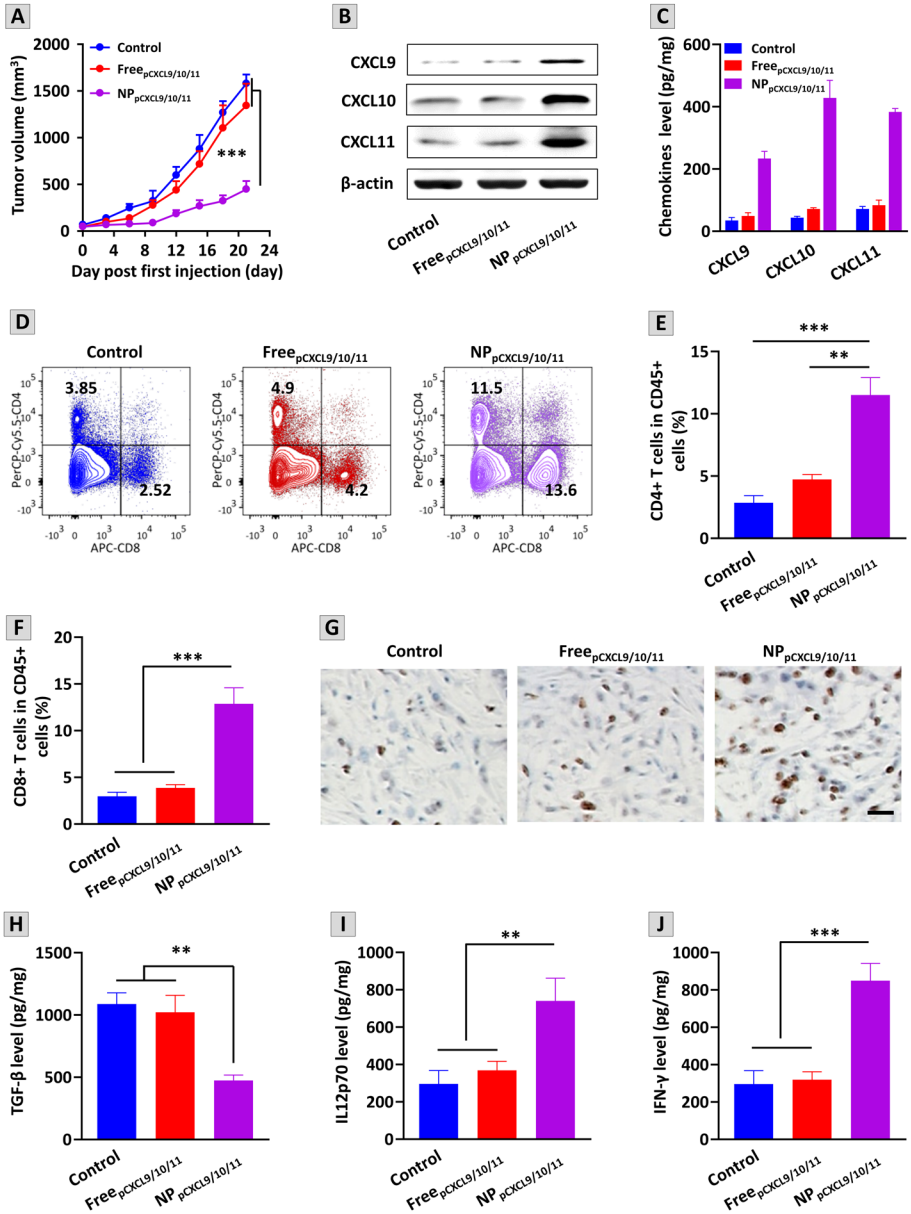

Fig. 4 NPpCXCL9/10/11 exhibits an efficient antitumor effect in the subcutaneous LLC tumor model. **A** Tumor growth curve. Subcutaneous LLC tumor model was established in C57BL/6 mice, and mice were intravenously treated with FreepCXCL9/10/11 or NPpCXCL9/10/11 every 3 days for 6 repeats when the tumor volumes reached about 50 mm^3, the equivalent injection dose of pCXCL9, pCXCL10, and pCXCL11 was 15 μg per mice. The levels of CXCL9, CXCL10, and CXCL11 in the tumor tissues were examined by western blot (**B**) and ELISA (**C**) at the end of the anti-tumor study. **D** Tumor tissues were digested and the ratios of CD4 + and CD8 + T cells in the CD45 + tumor-infiltrating immune cells were examined by multi-color flow cytometry. A representative flow cytometry image was shown. The percentages of CD4 + T cells (**E**) and CD8 + T cells (**F**) in CD45 + cells were calculated. **G** Distributions of T cells were evaluated by (2) of CD3. ELISA results of cytokines production in the tumors from mice receiving indicated treatments (**H**: TGF-β; **I**: IL12p70; **J**: IFN-γ). Data represent means ± SD. n = 6 mice, $^{**}p < 0.01$, $^{***}p < 0.001$

decreased in mice treated with $NP_{pCXCL9/10/11}$. Correlatively, we detected remarkably increased protein levels of CXCL9, CXCL10 and CXCL11 in tumor tissues (Fig. 4B, C) of mice treated with $NP_{pCXCL9/10/11}$. Correspondingly, significantly increased $CD4^+$ T cells (Fig. 4D, E) and $CD8^+$ T cells (Fig. 4D, F) were observed in tumor tissues from mice treated with $NP_{pCXCL9/10/11}$. Consistently, immunohistochemical staining demonstrated obviously increased $CD3^+$ T cells in tumor tissues of $NP_{pCXCL9/10/11}$-treated mice (Fig. 4G). Furthermore, there was no significant difference in TGF-β (Fig. 4H), IL-12 (Fig. 4I) and IFN-γ (Fig. 4J) levels in tumor tissues between non-treated and free pCXCL9/10/11-treated mice. In contrast, $NP_{pCXCL9/10/11}$-treated mice showed significantly decreased TGF-β (Fig. 4H) while significantly increased levels of IL-12 (Fig. 4I) and IFN-γ (Fig. 4J) in tumors when compared to non-treated and free pCXCL9/10/11-treated mice. There results showed that $NP_{pCXCL9/10/11}$ treatment promoted T cell infiltration in tumors and exhibited anti-tumor activity.

Anti-PD1 antibody significantly enhanced the anti-tumor efficacy of $NP_{pCXCL9/10/11}$

Programmed cell death protein 1 (PD1) is an inhibitory receptor expressed by T cells during activation, which significantly impairs the anti-tumor ability of T cells. Increasing evidence has suggested that anti-PD1 antibodies could significantly enhance the anti-tumor effect of T cells (Jiang et al. 2019). Therefore, we continued to investigate the potential effects of anti-PD1 antibody together with $NP_{pCXCL9/10/11}$ on tumors. Consistent to previous report, we observed obvious expression of PD-1 on $CD8^+$ T cells (Fig. 5A). Since $NP_{pCXCL9/10/11}$ promoted the infiltration of T cells in tumors, we also detected markedly increased PD1 expression in tumors from mice treated with $NP_{pCXCL9/10/11}$ (Fig. 5B). Both anti-PD1 antibody and $NP_{pCXCL9/10/11}$ treatment decreased the tumor volume (Fig. 5C), and mice treated with $NP_{pCXCL9/10/11}$ showed slightly reduced tumor volume when compared to mice treated with anti-PD1 antibody. Intriguingly, mice treated with the combination of anti-PD1 antibody and $NP_{pCXCL9/10/11}$ exhibited significantly reduced tumor volume when compared to mice with single treatment. Correspondingly, mice treated with anti-PD1 antibody or $NP_{pCXCL9/10/11}$ showed increased survival rate, while mice treated with the combination of anti-PD1 antibody and $NP_{pCXCL9/10/11}$ displayed the highest survival rate (Fig. 5D). Collectively, these results showed $NP_{pCXCL9/10/11}$ together with anti-PD1 antibody exhibited enhanced anti-tumor efficacy.

Discussion

In this study, we prepared nanoparticles containing plasmids expressing chemokines CXCL9, CXCL10 and CXCL11 and treated LLC cells with these nanoparticles. We found LLC cells treated with $NP_{pCXCL9/10/11}$ started to express these chemokines and promoted T cell invasion in vitro. In addition, we found $NP_{pCXCL9/10/11}$ decreased the tumor volume in mice and promoted the infiltration of both $CD4^+$ and $CD8^+$ T cells into tumors and elevated levels of both IL-12 and IFN-γ in tumors. Finally, we found that $NP_{pCXCL9/10/11}$ together with anti-PD-1 antibody displayed better anti-tumor effects. Therefore, our study demonstrated that overexpressing CXCL9, CXCL10 and CXCL11 in tumors exerted anti-tumor activity, suggesting overexpressing these chemokines could be used as therapeutic strategy for cancer treatment.

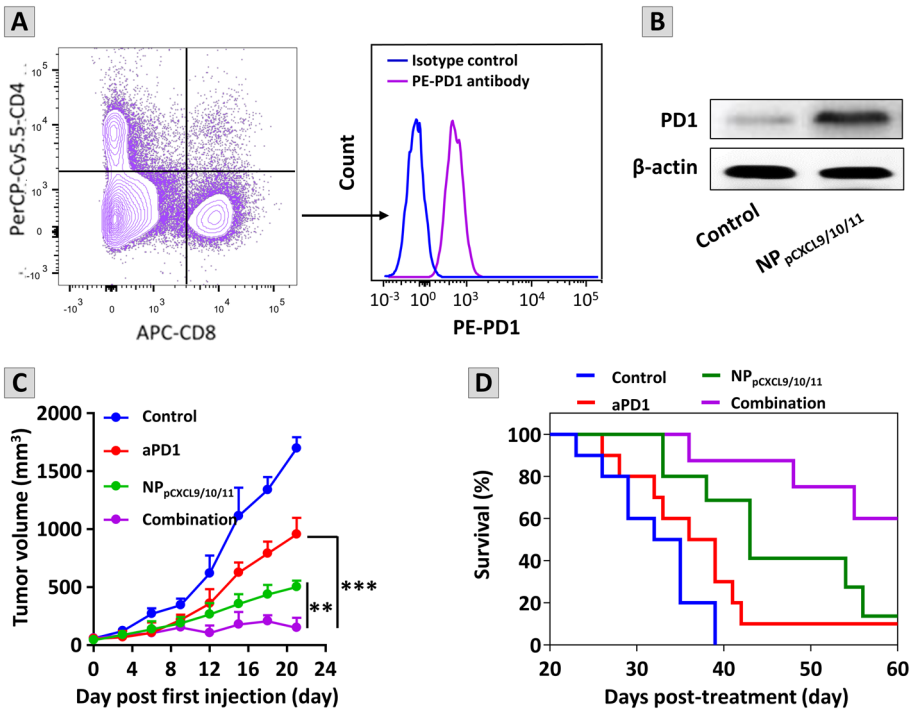

Fig. 5 Anti-PD1 antibody significantly enhances the anti-tumor efficacy of NPpCXCL9/10/11 of the LLC model. **A** PD1 expression of CD8 + T cells was examined by flow cytometry. **B** PD1 expression in tumor tissues was examined by western blot. **C** Tumor growth curve. Mice bearing LLC tumors were treated with aPD1, NPpCXCL9/10/11, or the combination. The equivalent injection dose of pCXCL9, pCXCL10, and pCXCL11 was 15 μg per mice, and the injection dose of aPD1 was 100 μg per mice. Data represent means ± SD. n = 10 mice, $^{**}p < 0.01$, $^{***}p < 0.001$. **D** Survival curve of mice bearing LLC tumors

Cancer immunotherapy based on immune checkpoint blockade (ICB) has led to significant and long-lasting clinical responses in patients with various cancers. However, the revolutionary achievement of ICB has been critically challenged by the observation that only a small proportion of patients show durable and continuous benefits from this therapy. The failure to attain durable clinical response might be caused by limited infiltration of immune cells into the tumor (Fares et al. 2019). In contrast, sufficient infiltration of T lymphocytes into the tumor microenvironment could predict the responses to T cell-based immunotherapies (Zhang et al. 2019). Therefore, researchers have focused on how to enhance T cell infiltration into tumor tissues to improve the efficacy of cancer immunotherapies (Oelkrug and Ramage 2014).

Chemokines, which are involved in the recruitment of lymphocytes, have been shown to affect specific T cell recruitment. CXCR3, the chemokine receptor expressed on T cells, has been shown to play a crucial role in the regulation of leucocyte migration to inflammatory sites (Hamann and Syrbe 2000). CXCR3 binds to its ligand CXCL9, CXCL10 and CXCL11 (Müller et al. 2010). The use of CXCR3 ligands to attract T cells into tumor sites has been shown to be an effective anti-tumor strategy. For example, Zhang and colleagues described that combination of CXCL9 expression and cisplatin enhanced the anti-tumor activity and augmented the inhibition of angiogenesis in both colon and lung cancers in mice (Zhang et al. 2006).

Intra-tumor injection of CXCL9 or CXCL10 reduced tumor growth and promoted mouse survival by enhancing the tumor infiltration of $CXCR3^+$ mononuclear cells (Pan et al. 2006; Arenberg et al. 2001). Using tumor-selective oncolytic vaccinia virus expressing CXCL11, Liu et al. demonstrated that expressing CXCL11 enhanced the therapeutic efficacy of the oncolytic viruses (Liu et al. 2016). In the present study, we administrated nanoparticles containing plasmids expressing CXCL9, CXCL10 and CXCL11 to tumors, which resulted in enhanced infiltration of both $CD4^+$ and $CD8^+$ T cells in tumors and decreased tumor size. Together with anti-PD-1 antibody, these nanoparticles displayed better anti-tumor activity, which suggested CXCR3/ligands system should synergize with anti-PD-1 therapy (Han et al. 2019).

PBAE nanoparticles have been widely utilized for delivery of low molecular weight drugs, oligonucleotides and plasmid DNA (Potineni et al. 2003; Little et al. 2004; Lynn et al. 2001). Compared to other nanoparticles, the PBAE nanoparticles have a cationic charge due to protonation of the tertiary amines of the polymer backbone, which is essential for effective intracellular delivery, as it is one of determinants for initial interaction between the delivery system and the cell surface (negatively charged) triggering the process of endocytosis (Potineni et al. 2003). In the present study, we also utilized these nanoparticles to deliver the plasmids encoding chemokines to cells or tumors. Compared to traditional transfection reagent Lipofectamine, PBAE nanoparticles displayed significantly higher efficiency, especially in the mouse tumor model. Besides PBAE nanoparticles, other nanoparticles have also been utilized as novel approach to deliver drugs to treat multiple diseases including cancer (Patra et al. 2018). Compared to conventional drug delivery, nanoparticles preferably accumulate at the tumor area due to the enhanced permeability and retention effect of the tumor (Maeda et al. 2013). In addition, nanoparticles can be modified to function as targeting agents when loaded with tumor targeting agents (Salahandish et al. 2018), as well as to modulate pathophysiology of tumor microenvironment (Wilson and Hay 2011). In the present study, we generated the common nanoparticles, and it would be interesting to modify these nanoparticles to gain even higher efficacy of anti-tumor effects.

Conclusions

In the present study, we found that nanoparticles efficiently delivered CXCL9/10/11 plasmid DNAs into cells and enabled the expression of these chemokines, which in LLC cells promoted infiltration of T cells in both in vitro and in vivo models. Nanoparticles displayed anti-tumor activity in mice, which was further synergized with anti-PD-1 antibody.

Methods

Polymer synthesis

Polymer 446 was synthesized as described previously (Rui et al. 2020). Briefly, monomer B4 and S4 were mixed and stirred overnight at 90 °C. On the next day, the B4–S4 polymer was dissolved in anhydrous tetrahydrofuran to a final concentration of 167 mg/mL. Then the polymer was incubated with 0.5 M monomer E6 at room temperature for 1 h. The polymer was washed with diethyl ether twice and subjected to vacuum desiccant

chamber to remove the solvent. The polymer was dissolved in DMSO and stored at − 20 °C.

Nanoparticle characterization

The diameter of nanoparticles was measured at the concentration of 1.0 mg/mL in PBS (pH 7.4) by DLS using Zetasizer NanoZS (Malvern PANalytical Products, Shanghai, China) at 25 °C. The morphology of nanoparticles was analyzed by SEM.

Plasmid construction

Murine CXCL9, CXCL10 and CXCL11 were amplified using mouse cDNA library as templates and cloned into pCDNA3.1 vector as described previously (Kumar et al. 2001).

Cell transfection

Lewis lung carcinoma (LLC) cells, a cell line in lung cancer research established from the lung of a C57BL mouse bearing a tumor resulting from an implantation of primary Lewis lung carcinoma, was widely used in lung cancer research. LLC cells were cultured in DMEM supplemented with 10% heat-inactivated fetal bovine serum (FBS, Gibco). For transfection, LLC cells (2×10^5 cells/well) were seeded in six-well plates for 24 h and then incubated with free plasmid pEGFP-N2, $Lipo_{pEGFP\text{-}N2}$ or $NP_{pEGFP\text{-}N2}$ at the dose of 0.5 nM, and the expression of GFP was monitored using flow cytometry and fluorescence microcopy 48 h post transfection.

Western blot

Total proteins from cells and tumor tissues were extracted using RIPA lysis buffer and then subjected to western blot following standard protocols. Primary antibodies used in this study included: anti-CXCL9 (1:1000, Abcam), anti-CXCL10 (1:500, Abcam), anti-CXCL11 (1:1000. Thermo Fisher), anti-β actin (1:2000, Abcam).

ELISA

The quantity of CXCL9, CXCL10, CXCL11 in cell culture supernatant of LLC cells and in homogenate of tumor tissues, the TGF-β, IL-12 p70 and IFN-γ in homogenate of tumor tissues were measured using specific ELISA kits (Abcam) following manufacturer's instructions.

T cell invasion assay

T cell invasion was detected using 5.0 μm pore size Transwell plate (Costar, Cambridge, MA). T cells were purified from spleen using Pan T Cell Isolation Kit II (Miltenyi Biotec). 1×10^5 T cells were placed in the top chamber of the Transwell, while LLC cells were seeded in the bottom of wells, and T cells were transfected as mentioned above. After 48 h incubation, the T cell numbers in lower chamber were counted.

Flow cytometry

$CD4^+$ and $CD8^+$ T cells were purified using $CD4^+$ T Cell Isolation Kit and $CD8^+$ T cell Isolation Kit (Miltenyi Biotec), respectively. Tumor tissues were harvested, minced and then digested with collagenase and DNase (Sigma-Aldrich, St. Louis, MO) to acquire

single cell suspension. Cells were suspended in staining buffer (2% FBS in PBS) and incubated with fluorescent-labeled antibodies (working concentration at 0.5 μg/mL) on ice for 30 min. After wash, cells were subjected to BD LSR flow cytometry for analysis. The data was analyzed using FlowJo.

Mice LLC model

LLC cells were injected subcutaneously into one flank of C57BL/6 mice as described previously (Keane et al. 2004). Tumor volume was measured at different timepoints. When tumor volumes reached about 50 mm^3, mice were intravenously injected with free plasmids (15 μg/mouse), $NP_{pCXCL9/10/11}$ (15 μg/mouse), anti-PD-1 (100 μg/mouse), or $NP_{pCXCL9/10/11}$ together with anti-PD-1 every 3 days for 6 repeats. Animal studies were approved by Cangzhou Central Hospital.

Immunohistochemical staining

Tumor tissues were harvested, fixed and embedded in paraffin. The tissue blocks were cut into slides. The staining was performed following the standard protocol (Abcam).

Statistical analysis

The data were presented as mean ± standard deviation (SD). One or two-way analysis of variance (ANOVA) and appropriate post hoc test were used for analysis. When $p < 0.05$, the difference was considered as significant.

Abbreviations

NSCLC: Non-small cell lung cancer; ICP: Immune checkpoints; THF: Tetrahydrofuran; DLS: Dynamic light scattering; SEM: Scanning electron microscope; LLC: Lewis lung cancer; SD: Standard deviation; ANOVA: Analysis of variance; ICB: Immune checkpoint blockade (ICB); EPR: Enhanced permeability and retention.

Supplementary Information

The online version contains supplementary material available at https://doi.org/10.1186/s12645-022-00116-z.

Additional file 1. Figure S1. Chemical structure (A) and FTIR spectra of PBAE (B).

Acknowledgements

None.

Author contributions

All authors performed experiments and analysed data. Yuxia Ma and Yi Liu wrote the manuscript and manuscript revisions. All authors read and approved the final manuscript.

Funding

This study was supported by Cangzhou Science and Technology Research and Development Program (204106108).

Availability of data and materials

Original data could be accessed upon reasonable request.

Declarations

Ethics approval and consent to participate

Animal research was approved by the institutional animal care and use committee of Cangzhou Central Hospital.

Consent for publication

Not appliable.

Competing interests

The authors declare that they have no known competing interests.

Author details
[1]Department of Internal Medicine, Cangzhou Central Hospital, 6 Xinhua WestRoad, Cangzhou 061001, Heibei, China.
[2]Cangzhou Prison, No.47 Hexi NorthStreet, Cangzhou 061001, Heibei, China.

Received: 12 October 2021 Accepted: 9 April 2022
Published online: 25 April 2022

References

Arenberg DA, White ES, Burdick MD, Strom SR, Strieter RM (2001) Improved survival in tumor-bearing SCID mice treated with interferon-gamma-inducible protein 10 (IP-10/CXCL10). Cancer Immunol Immunother 50:533–538. https://doi.org/10.1007/s00262-001-0231-9

Bonaventura P, Shekarian T, Alcazer V, Valladeau-Guilemond J, Valsesia-Wittmann S, Amigorena S, Caux C, Depil S (2019) Cold tumors: a therapeutic challenge for immunotherapy. Front Immunol 10:168. https://doi.org/10.3389/fimmu.2019.00168

Chow MT, Ozga AJ, Servis RL, Frederick DT, Lo JA, Fisher DE, Freeman GJ, Boland GM, Luster AD (2019) Intratumoral activity of the CXCR3 chemokine system is required for the efficacy of anti-PD-1 therapy. Immunity 50:1498-1512.e1495. https://doi.org/10.1016/j.immuni.2019.04.010

Dela Cruz CS, Tanoue LT, Matthay RA (2011) Lung cancer: epidemiology, etiology, and prevention. Clin Chest Med 32:605–644. https://doi.org/10.1016/j.ccm.2011.09.001

Fares CM, Van Allen EM, Drake CG, Allison JP, Hu-Lieskovan S (2019) Mechanisms of resistance to immune checkpoint blockade: why does checkpoint inhibitor immunotherapy not work for all patients? Am Soc Clin Oncol Educ Book 39:147–164. https://doi.org/10.1200/edbk_240837

Fujita M, Zhu X, Ueda R, Sasaki K, Kohanbash G, Kastenhuber ER, McDonald HA, Gibson GA, Watkins SC, Muthuswamy R, Kalinski P, Okada H (2009) Effective immunotherapy against murine gliomas using type 1 polarizing dendritic cells–significant roles of CXCL10. Cancer Res 69:1587–1595. https://doi.org/10.1158/0008-5472.CAN-08-2915

Groom JR, Luster AD (2011) CXCR3 in T cell function. Exp Cell Res 317:620–631. https://doi.org/10.1016/j.yexcr.2010.12.017

Hamann A, Syrbe U (2000) T-cell trafficking into sites of inflammation. Rheumatology (oxford) 39:696–699. https://doi.org/10.1093/rheumatology/39.7.696

Han X, Wang Y, Sun J, Tan T, Cai X, Lin P, Tan Y, Zheng B, Wang B, Wang J, Xu L, Yu Z, Xu Q, Wu X, Gu Y (2019) Role of CXCR3 signaling in response to anti-PD-1 therapy. EBioMedicine 48:169–177. https://doi.org/10.1016/j.ebiom.2019.08.067

Harlin H, Meng Y, Peterson AC, Zha Y, Tretiakova M, Slingluff C, McKee M, Gajewski TF (2009) Chemokine expression in melanoma metastases associated with CD8+ T-cell recruitment. Cancer Res 69:3077–3085. https://doi.org/10.1158/0008-5472.CAN-08-2281

Huang Y, Li L, Liu W, Tang T, Chen L (2020) The progress of CAR-T therapy in cancer and beyond. Stemedicine 1:e47. https://doi.org/10.37175/stemedicine.v1i3.47

Jiang Y, Chen M, Nie H, Yuan Y (2019) PD-1 and PD-L1 in cancer immunotherapy: clinical implications and future considerations. Hum Vaccin Immunother 15:1111–1122. https://doi.org/10.1080/21645515.2019.1571892

Keane MP, Belperio JA, Xue YY, Burdick MD, Strieter RM (2004) Depletion of CXCR2 inhibits tumor growth and angiogenesis in a murine model of lung cancer. J Immunol 172:2853–2860. https://doi.org/10.4049/jimmunol.172.5.2853

Kim ES (2016) Chemotherapy resistance in lung cancer. Adv Exp Med Biol 893:189–209. https://doi.org/10.1007/978-3-319-24223-1_10

Kumar M, Behera AK, Hu J, Lockey RF, Mohapatra SS (2001) IFN-gamma and IL-12 plasmid DNAs as vaccine adjuvant in a murine model of grass allergy. J Allergy Clin Immunol 108:402–408. https://doi.org/10.1067/mai.2001.117261

Little SR, Lynn DM, Ge Q, Anderson DG, Puram SV, Chen J, Eisen HN, Langer R (2004) Poly-beta amino ester-containing microparticles enhance the activity of nonviral genetic vaccines. Proc Natl Acad Sci U S A 101:9534–9539. https://doi.org/10.1073/pnas.0403549101

Liu Z, Ravindranathan R, Li J, Kalinski P, Guo ZS, Bartlett DL (2016) CXCL11-Armed oncolytic poxvirus elicits potent antitumor immunity and shows enhanced therapeutic efficacy. Oncoimmunology 5:e1091554. https://doi.org/10.1080/2162402x.2015.1091554

Luster AD (1998) Chemokines–chemotactic cytokines that mediate inflammation. N Engl J Med 338:436–445. https://doi.org/10.1056/NEJM199802123380706

Luster AD, Leder P (1993) IP-10, a -C-X-C- chemokine, elicits a potent thymus-dependent antitumor response in vivo. J Exp Med 178:1057–1065. https://doi.org/10.1084/jem.178.3.1057

Lynn DM, Amiji MM, Langer R (2001) pH-Responsive Polymer Microspheres: Rapid Release of Encapsulated Material within the Range of Intracellular pH Financial support was provided by the NSF (Cooperative Agreement No. ECC9843342 to the MIT Biotechnology Process Engineering Center), the NIH (GM26698), and the Department of the Army (Cooperative Agreement DAMD 17–99-2-9-001 to the Center for Innovative Minimally Invasive Therapy). D.M.L. wishes to thank the NIH for a Postdoctoral Fellowship (NRSA Fellowship No. 1 F32 GM20227-01). Scanning electron microscopy and confocal microscopy images were acquired by William Fowle at the Northeastern University Center for Electron Microscopy. Dr. David Putnam, David Ting, and Tommy Thomas are thanked for helpful discussions. Angew Chem Int Ed Engl 40:1707–1710

Maeda H, Nakamura H, Fang J (2013) The EPR effect for macromolecular drug delivery to solid tumors: Improvement of tumor uptake, lowering of systemic toxicity, and distinct tumor imaging in vivo. Adv Drug Deliv Rev 65:71–79. https://doi.org/10.1016/j.addr.2012.10.002

Massarelli E, Papadimitrakopoulou V, Welsh J, Tang C, Tsao AS (2014) Immunotherapy in lung cancer. Transl Lung Cancer Res 3:53–63. https://doi.org/10.3978/j.issn.2218-6751.2014.01.01

Mikucki ME, Fisher DT, Matsuzaki J, Skitzki JJ, Gaulin NB, Muhitch JB, Ku AW, Frelinger JG, Odunsi K, Gajewski TF, Luster AD, Evans SS (2015) Non-redundant requirement for CXCR3 signalling during tumoricidal T-cell trafficking across tumour vascular checkpoints. Nat Commun 6:7458. https://doi.org/10.1038/ncomms8458
Miller KD, Siegel RL, Lin CC, Mariotto AB, Kramer JL, Rowland JH, Stein KD, Alteri R, Jemal A (2016) Cancer treatment and survivorship statistics, 2016. CA Cancer J Clin 66:271–289. https://doi.org/10.3322/caac.21349
Müller M, Carter S, Hofer MJ, Campbell IL (2010) Review: The chemokine receptor CXCR3 and its ligands CXCL9, CXCL10 and CXCL11 in neuroimmunity–a tale of conflict and conundrum. Neuropathol Appl Neurobiol 36:368–387. https://doi.org/10.1111/j.1365-2990.2010.01089.x
Oelkrug C, Ramage JM (2014) Enhancement of T cell recruitment and infiltration into tumours. Clin Exp Immunol 178:1–8. https://doi.org/10.1111/cei.12382
Pan J, Burdick MD, Belperio JA, Xue YY, Gerard C, Sharma S, Dubinett SM, Strieter RM (2006) CXCR3/CXCR3 ligand biological axis impairs RENCA tumor growth by a mechanism of immunoangiostasis. J Immunol 176:1456–1464. https://doi.org/10.4049/jimmunol.176.3.1456
Patra JK, Das G, Fraceto LF, Campos EVR, Rodriguez-Torres MDP, Acosta-Torres LS, Diaz-Torres LA, Grillo R, Swamy MK, Sharma S, Habtemariam S, Shin HS (2018) Nano based drug delivery systems: recent developments and future prospects. J Nanobiotechnol 16:71. https://doi.org/10.1186/s12951-018-0392-8
Potineni A, Lynn DM, Langer R, Amiji MM (2003) Poly(ethylene oxide)-modified poly(beta-amino ester) nanoparticles as a pH-sensitive biodegradable system for paclitaxel delivery. J Control Release 86:223–234. https://doi.org/10.1016/s0168-3659(02)00374-7
Rui Y, Varanasi M, Mendes S, Yamagata HM, Wilson DR, Green JJ (2020) Poly(Beta-Amino Ester) Nanoparticles Enable Non-viral Delivery of CRISPR-Cas9 Plasmids for Gene Knockout and Gene Deletion. Mol Ther Nucleic Acids 20:661–672. https://doi.org/10.1016/j.omtn.2020.04.005
Salahandish R, Ghaffarinejad A, Naghib SM, Majidzadeh AK, Zargartalebi H, Sanati-Nezhad A (2018) Nano-biosensor for highly sensitive detection of HER2 positive breast cancer. Biosens Bioelectron 117:104–111. https://doi.org/10.1016/j.bios.2018.05.043
Sosa Iglesias V, Giuranno L, Dubois LJ, Theys J, Vooijs M (2018) Drug resistance in non-small cell lung cancer: a potential for NOTCH Targeting? Front Oncol 8:267. https://doi.org/10.3389/fonc.2018.00267
Tang H, Wang Y, Chlewicki LK, Zhang Y, Guo J, Liang W, Wang J, Wang X, Fu YX (2016) Facilitating T Cell infiltration in tumor microenvironment overcomes resistance to PD-L1 Blockade. Cancer Cell 29:285–296. https://doi.org/10.1016/j.ccell.2016.02.004
Wilson WR, Hay MP (2011) Targeting hypoxia in cancer therapy. Nat Rev Cancer 11:393–410. https://doi.org/10.1038/nrc3064
Zhang R, Tian L, Chen LJ, Xiao F, Hou JM, Zhao X, Li G, Yao B, Wen YJ, Li J, Zhang L, Chen XC, Luo F, Peng F, Jiang Y, Wei YQ (2006) Combination of MIG (CXCL9) chemokine gene therapy with low-dose cisplatin improves therapeutic efficacy against murine carcinoma. Gene Ther 13:1263–1271. https://doi.org/10.1038/sj.gt.3302756
Zhang J, Endres S, Kobold S (2019) Enhancing tumor T cell infiltration to enable cancer immunotherapy. Immunotherapy 11:201–213. https://doi.org/10.2217/imt-2018-0111

Publisher's Note